

MECHANICS AND MATERIALS IN DESIGN

**THEORY, EXPERIMENTS AND APPLICATIONS
IN ENGINEERING AND BIOMECHANICS**

Editors

J.F. Silva Gomes

Shaker A. Meguid

*ABSTRACTS M2D2022 - 9TH INTERNATIONAL CONFERENCE ON MECHANICS AND
MATERIALS IN DESIGN, FUNCHAL/PORTUGAL, 26-30 JUNE 2022*

**INEGI-FEUP
(2022)**

PAPER REF: 18321

NEW DEVELOPMENTS ON THE BENDING RESISTANCE IN COMPOSITE SLABS WITH STEEL DECK UNDER FIRE

Paulo A.G. Piloto^{1(*)}, Matheus Bez da Silveira², Carlos Balsa³, Gustavo Lacerda Dias⁴

¹INEGI/LAETA, Instituto Politécnico de Bragança (IPB), Bragança, Portugal

²Instituto Politécnico de Bragança (IPB), Bragança, Portugal

³Instituto Politécnico de Bragança (IPB), Bragança, Portugal

⁴DACOC, Dep. of Civil Construction, Federal Tech. University of Paraná (UTFPR), Pato Branco, Brasil

^(*)Email: ppiloto@ipb.pt

ABSTRACT

The main objective of this work is to investigate the fire effect on the bending resistance of the composite slab with steel deck, comparing the behavior of Normal Weight Concrete (NWC) and Light Weight Concrete (LWC), when submitted to standard fire. The bending resistance of these two composite slabs is affected, primarily, by their mechanical properties, but also by their thermal properties [1][2]. The analysis is based on a finite element model, used to solve the non-linear transient analysis of composite slabs. Based on the average temperature of each component, the reduction load bearing capacity is determined, for specific fire ratings (R30, R60, R90 and R120). The numerical models are simulated using the ANSYS and MATLAB software, to verify the effect of using different modelling techniques.

Keywords: composite slabs, standard fire, normal weight concrete, lightweight concrete, numerical model.

INTRODUCTION

Composite steel and concrete slabs can be considered as a mix of a reinforced concrete layer located over a profiled steel deck, which may or may not be reinforced by steel bars located between its ribs. This configuration provides good bending resistance under positive moments (sagging) and negative moments (hogging). A steel mesh is normally used on the top of the concrete layer to minimize concrete cracking. The use of composite slabs provides a high performance in bending resistance to large loads and can be considered a good solution for large spans, such as commercial or office buildings, hospitals, parking lots, etc. In these cases, the use of composite slabs aggregates economic advantages, such as: a reduction cost due to the use of less material and a reduction in construction time due to the pre-fabrication of the steel deck used for formwork.

The Eurocode EN1994-1.2 [1], provides design rules for the fire safety analysis of composite slabs with steel deck. This standard presents a simplified calculation model that makes possible to determine the sagging moment. However, since the last review was made, more than fifteen years ago, the methodology does not take into consideration some important events that occur during the fire exposure of the slab, such as the debonding effect. This event has been identified by several researchers [3][4][5][6][7] and may be justified by the existence of the thermal bowing and the existence of different thermal expansion coefficients between steel and concrete.

According to previous investigations, the debonding is responsible for an extra thermal resistance that contributes for a temperature variation in the composite slab. This event that can

be predicted by the consideration of an air gap layer between the steel deck and the concrete. Another parameter that is not considered on the simplified model is the influence that the thickness (h_1) of the concrete, located above the steel deck upper flange, has in the calculation of the temperature of each component. This effect can also be affecting the position of the plastic neutral axis position of the slab. After all, this thickness contributes effectively to the internal heat flow pattern of the slabs, affecting the steel components (bottom flange, web, upper flange rebars) and concrete temperatures, and consequently, the reduction coefficients used for calculating the sagging moment.

RESULTS AND CONCLUSIONS

In order to optimize the calculation model presented by Eurocode 1994 1-2 [1], a parametric study was performed by analyzing the effect of different types of concrete, different concrete thicknesses and four different types of steel decks (trapezoidal and re-entrant). In this study, two trapezoidal steel decks were used (Confraplus 60 and Polydeck 59s), adopting different concrete thickness (50, 70, 90, 110 and 125 mm), and two re-entrant steel decks were also used (Multideck 50 and Bondek) with concrete thicknesses of 60, 70, 90, 110 and 125 mm.

A comparison between the results obtained through the numerical models and the values obtained through the analytical method is presented. These results highlight the difference between the two solution methods, which means that a new formula should be presented for the calculation method in Eurocode EN1994-1.2.

REFERENCES

- [1] CEN- European Committee for Standardization, EN 1994-1-2: Design of composite steel and concrete structures. Part 1-2: General rules - Structural fire design. Brussels: CEN-European Committee for Standardization, 2005.
- [2] M. Malik, S. K. Bhattacharyya, and S. V. Barai, "Thermal and mechanical properties of concrete and its constituents at elevated temperatures: A review," *Construction and Building Materials*, vol. 270, p.121398, 2020, doi: 10.1016/j.conbuildmat.2020.121398.
- [3] P. A. G. Piloto, C. Balsa, L. M. C. Santos, and É. F. A. Kimura, "Effect of the load level on the resistance of composite slabs with steel decking under fire conditions," *Journal of Fire Sciences*, vol. 38, no. 2, pp. 212–231, 2020, doi: 10.1177/0734904119892210.
- [4] P. A. G. Piloto, C. Balsa, F. Ribeiro, and R. Rigobello, "Computational Simulation of the Thermal Effects on Composite Slabs Under Fire Conditions," *Mathematics in Computer Science*, 2020, doi: 10.1007/s11786-020-00466-0.
- [5] J. Jiang, A. Pintar, J. M. Weigand, J. A. Main, and F. Sadek, "Improved calculation method for insulation-based fire resistance of composite slabs," *Fire Safety Journal*, vol. 105, pp.144–153, Mar. 2019, doi: 10.1016/J.FIRESAF.2019.02.013.
- [6] P. A. G. Piloto, C. Balsa, F. Ribeiro, L. Santos, R. Rigobello, and É. Kimura, "Three-Dimensional Numerical Modelling of Fire Exposed Composite Slabs With Steel Deck," *MATTER: International Journal of Science and Technology*, vol. 5, no. 2, pp.48–67, 2019, doi: 10.20319/mijst.2019.52.4867.
- [7] J. Jiang, J. A. Main, J. M. Weigand, and F. H. Sadek, "Thermal performance of composite slabs with profiled steel decking exposed to fire effects," *Fire Safety Journal*, vol. 95, no. May 2017, pp.25–41, 2018, doi: 10.1016/j.firesaf.2017.10.003.

PROCEEDINGS M2D2022

9th International Conference MECHANICS AND MATERIALS IN DESIGN

Funchal/Portugal, 26-30 June 2022

Editors

J.F. Silva Gomes | Shaker A. Meguid

ISBN: 978-989-54756-3-6

INEGI-FEUP
(2022)

ENTER

PAPER REF: 18321

NEW DEVELOPMENTS ON THE BENDING RESISTANCE IN COMPOSITE SLABS WITH STEEL DECK UNDER FIRE

Paulo A.G. Piloto^{1(*)}, Matheus Bez da Silveira², Carlos Balsa³, Gustavo Lacerda Dias⁴

¹INEGI/LAETA, Instituto Politécnico de Bragança (IPB), Bragança, Portugal

²Instituto Politécnico de Bragança (IPB), Bragança, Portugal

³Instituto Politécnico de Bragança (IPB), Bragança, Portugal

⁴DACOC, Dep. of Civil Construction, Federal Tech. University of Paraná (UTFPR), Pato Branco, Brasil

(*)Email: ppiloto@ipb.pt

ABSTRACT

This work investigates the fire effect on the bending resistance of the composite slab reinforced with steel deck, comparing the behavior of Normal Weight Concrete (NWC) and Light Weight Concrete (LWC) during a standard fire ISO834. This analysis is required for structures in fire and is mainly affected by two factors: the thermal and mechanical properties of the materials. The results of the simplified method are compared with the numerical results obtained by a two-dimensional and a three-dimensional thermal analysis, with regards to the temperature effect from each component in to the bending resistance of the composite slab. This analysis consists of a non-linear transient thermal analysis using the finite element method, using two different software: ANSYS and MATLAB. Based on the average temperature of each component, new coefficients and a new proposal for annex D of Eurocode 1994-1.2 are presented. The reduction of the load bearing capacity is also determined.

Keywords: composite slabs, standard fire, normal weight concrete, lightweight concrete.

INTRODUCTION

Composite steel and concrete slabs are an alternative construction element characterised by a reinforced concrete layer located above the profiled steel deck, which may or may not be reinforced by steel bars. This structural element, see Figure 1, enhances the reduction of the self-weight of the structures, resistance against the concrete shrinkage (due to the contribution given by the steel mesh) while speeding up the construction process.

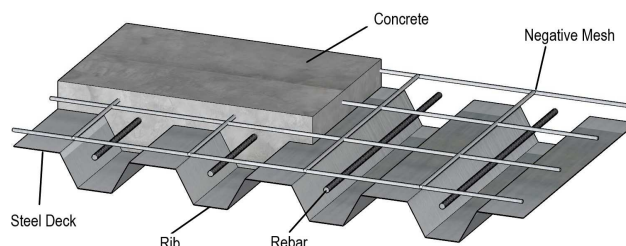


Fig. 1 – Steel/Concrete slab configuration.

The composite slabs are made of a profiled steel deck, which can also be used as permanent formwork. The use of composite slabs in buildings has become very popular in North America since 1960. However, due to the insufficient information regarding its structural safety, only after 1980 has become popular in Europe [1]. The thickness and geometry of the steel deck depend on the producer of the steel profiles, and usually includes a zinc coating on the exposed surface to enhance the corrosion resistance.

Although the composite slabs have numerous advantages, their behavior under fire conditions or when exposed to extreme climatic conditions requires special attention. Both situations are related to the steel deck's exposure. The corrosion problem caused mainly by the weather condition can be minimised by applying a zinc coat on the steel deck exposed surface [2], but the exposure to fire conditions generates internal forces in the slab which can reduce the structural integrity of the element. This investigation deals with the bending behaviour of the composite slab under a positive moment (sagging moment) and under fire conditions. The direct exposure of steel to fire leads to a reduction in its mechanical properties, thus, it is essential to specify the minimum fire resistance time in composite slabs aiming to avoid structural problems or the collapse of the element.

The current version of the Eurocode 1994-1.2 [3] presents a simplified calculation model to determine the bending resistance under fire, being responsible to provide fire safety for common fire rating times. However, since the last review was made, more than fifteen years ago, the methodology neglects some important effects during the fire exposure, such as the debonding effect and the concrete thickness above the steel deck.

This investigation enhances the analytical temperature calculation presented by the simplified calculation method, provided in the Annex D of Eurocode 1994 1-2, including a parametric analysis. The numerical models have already been validated by Paulo Piloto *et al.* [4-6]. The temperature field along the composite slabs using normal weight and lightweight concrete (NWC and LWC) is determined to four different types of steel deck geometries, trapezoidal and re-entrant, using different concrete thicknesses over the steel deck.

The numerical results obtained by two-dimensional and three-dimensional analyses were then compared against the Simplified Calculation Method and a new analytical calculation proposal, as well as new coefficients for the Annex D of Eurocode 1994-1-2, are presented. So, It is worth mentioning that this analysis highlights the improvement provided by the new proposal, both in estimating temperatures and the load-bearing (bending resistant) of composite slabs under fire conditions.

METHODS

The current design rules are based on two data sets: the thermal properties to perform the thermal analysis and the mechanical properties to perform the structural analysis. The thermal analysis depends on the thermal conductivity (λ), specific heat (C_p), and density (ρ), which are part of the energy equation, Eq. 1, that is necessary to solve. The boundary condition in the exposed side is governed by the convection and radiation heat flux, assuming the bulk temperature following the standard temperature, according to the ISO-834, see Eq. 2. The boundary conditions in the unexposed side may be governed by the convection heat flux, see Eq. 3, using the bulk temperature equal to 20°C. The Thermal analysis is incremental and iterative, using the convergence criterion in each time-step based on the heat flow, with a tolerance of 10^{-3} and reference value 10^{-6} . The mechanical analysis is simplified and depends on the reduction factors, determined based on the average temperature for each component (lower flange, web, upper flange, and rebars), see Eqs. 5 and 6.

$$\rho_{(T)} C_{p(T)} \frac{\partial T}{\partial t} = \nabla(\lambda_{(T)} \nabla T) \quad (1)$$

$$\lambda_{(T)} \nabla T \cdot \vec{n} = \alpha_c (T_\infty - T) + \phi \epsilon_m \epsilon_f \sigma (T_\infty^4 - T^4) \quad (2)$$

$$\lambda_{(T)} \nabla T \cdot \vec{n} = \alpha_c (T_\infty - T) \quad (3)$$

Once the heat flux by conduction on the composite slab depends on the material thermal properties, which change along the time, Eq. 1 is time-dependent and holds a transient thermal state. Moreover, the exposed boundary conditions also change with time and bulk temperature. So, in order to determine the temperature field along the time, the solution of Eq. 1 is required. The mechanical analysis method is based on the specification of the fire rating required for each composite slab. So, after determining the temperatures in each component, the next step is the determination of the slab plastic neutral axis following Eq. 5. It is worth mentioning that design rules are being applied only on simply supported slabs, exposed to standard fire ISO-834 [7], and under positive bending moments (sagging moment).

$$\sum_{i=1}^n A_i k_{y,\theta,i} \left(\frac{f_{y,i}}{\gamma_{M,fi,a}} \right) + \alpha_{slab} \sum_{j=1}^m A_j k_{c,\theta,j} \left(\frac{f_{c,j}}{\gamma_{M,fi,c}} \right) = 0 \quad (5)$$

Where $f_{y,i}$ is the yield stress associated with the steel element with an area A_i . This value should be considered positive if it is in the compressed region, and negative otherwise, $f_{c,j}$ is the concrete compressive strength at 20°C for the area A_j , considered above the neutral axis, α_{slab} is the reduction coefficient regarding the consideration of a concrete rectangular stress block, with a value of 0.85. The reduction coefficients $k_{y,\theta,i}$ are presented in Table 1. The reduction coefficient $k_{c,\theta,j}$ is assumed equal to 1.

Table 1 - Reduction Coefficients.

Temperature [°C]	$k_{p0,2,\theta}$	$k_{y,\theta}$	$k_{c,\theta}$
20	1.000	1.000	1.000
100	1.000	1.000	1.000
200	0.890	1.000	0.950
300	0.780	1.000	0.850
400	0.650	0.940	0.750
500	0.530	0.670	0.600
600	0.300	0.400	0.450
700	0.130	0.120	0.300
800	0.070	0.110	0.150
900	0.050	0.080	0.080
1000	0.030	0.050	0.040
1100	0.020	0.030	0.010
1200	0.000	0.000	0.000

The design bending moment resistance $M_{fi,t,Rd}$ (positive) can be determined using Eq. 6.

$$M_{fi,t,Rd} = \sum_{i=1}^n A_i z_i k_{y,\theta,i} \left(\frac{f_{y,i}}{\gamma_{M,fi,a}} \right) + \alpha_{slab} \sum_{j=1}^m A_j z_j k_{c,\theta,j} \left(\frac{f_{c,j}}{\gamma_{M,fi,c}} \right) \quad (6)$$

Where z_i and z_j represent the distance from the neutral axis to the respective geometric centres of the areas A_i and A_j .

THERMAL AND MECHANICAL MATERIAL PROPERTIES

The thermal properties of the materials that compose the slabs are temperature dependent, and are determined by the Eurocodes. Once the non-linearity of heat transfer is an intrinsic and important characteristic, the thermal properties of materials must be carefully incorporated into the numerical models. The Eurocodes 1992-1-2 [8], 1994-1-2 [3] and, 1993-1.2 [9] were adopted to determine the thermal properties of normal weight concrete, lightweight concrete and steel, respectively. The air thermal properties are based on Yunus A. experimental work [10]. Figures 2 – 5 depict the main thermal properties used in the numerical models.

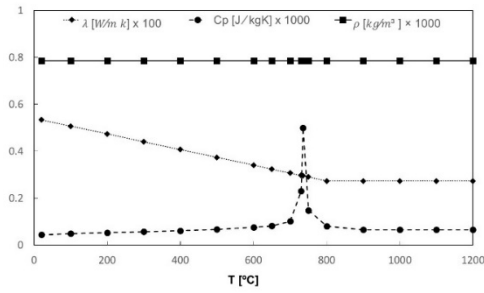


Fig. 2 – Steel Thermal Properties.

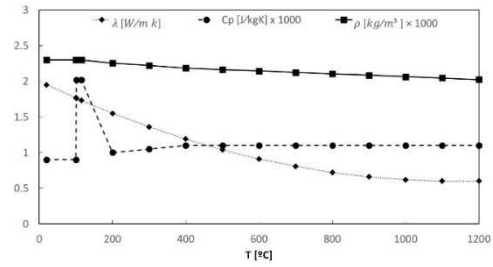


Fig. 3 – NWC Thermal Properties.

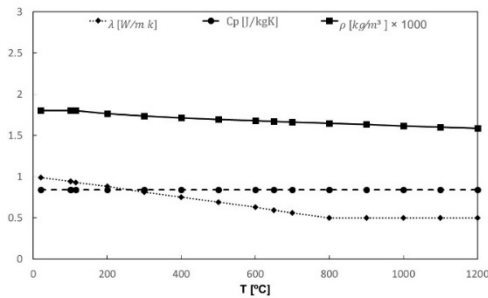


Fig. 4 – LWC Thermal Properties.

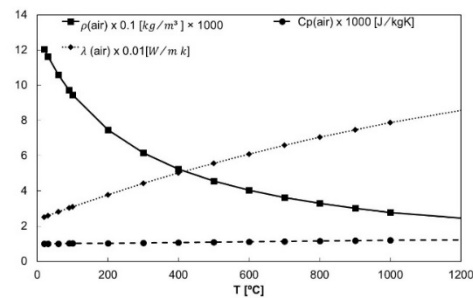


Fig. 5 – Air Thermal Properties.

The steel and concrete mechanical properties are also temperature dependents. For this reason, the temperature effect on the design strength should be considered in order to determine the load bearing capacity. The reduction coefficients for the steel deck strength are determined by $k_{p0,2,\theta}$ while the reduction coefficient for the strength of the rebars is determined by $k_{y,\theta}$. The reduction coefficients for the compressive strength of concrete ($k_{c,\theta}$) may be determined from Eurocode 1992-1-2, but in this case (component) it is set to 1. These coefficients are presented in Table 1.

PARAMETRIC ANALYSIS

The transient heat transfer analysis will be made on four different composite slabs with different geometries, as presented in Figures 6-9. Two trapezoidal geometries, and two re-entrant geometries were selected: Confraplus 60 and Polydeck 59s, Multideck 50, and Bondek. The thermal behavior of each of the four composite slabs is determined for different thicknesses of the concrete topping h_1 (thickness of the slab above the ribs). For trapezoidal geometries, the h_1 thicknesses were considered equal to 50, 70, 90, 110, and 125 mm. For the re-entrant geometries, the following thicknesses h_1 were considered: 60, 70, 90, 110, and 125 mm.

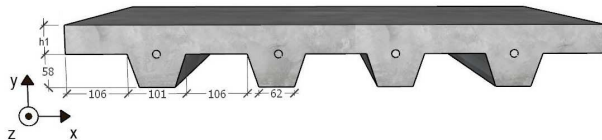


Fig. 6 – Confraplus 60 geometric characteristics.

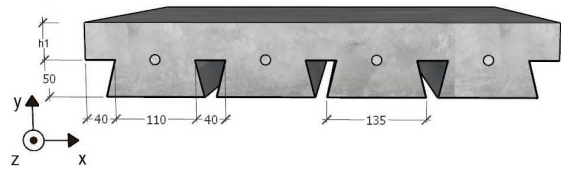


Fig. 7 – Multideck 50 geometric characteristics.

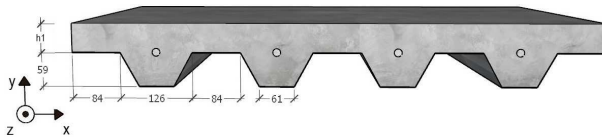


Fig. 8 – Polydeck 59S geometric characteristics.

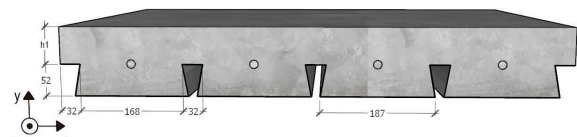


Fig. 9 – Bondek geometric characteristics.

The heat flux received by the exposed steel deck surface depends on the composite slab's view factor (φ), which changes according to each slab geometry. These values are presented in Table 2.

Table 2 – View Factor values.

Slab Geometry	Deck Component	View Factor (φ)
Confraplus 60	Upper flange	0.73
	Web	0.56
	Lower flange	1.00
Polydeck 59S	Upper flange	0.75
	Web	0.64
	Lower flange	1.00
Multideck 50	Upper flange	0.14
	Web	0.09
	Lower flange	1.00
Bondek	Upper flange	0.12
	Web	0.09
	Lower flange	1.00

ADVANCED CALCULATION METHOD

The advanced calculation method aims to determine the thermal response to fire, using the finite element method. The general procedure of the finite element method for solving Eq. 1 is based on the weak-form Galerkin model and from the minimum condition for the weighted residual method, leading to the matrix format of the energy equation (Eq. 7):

$$C_{(T^{n+1})} \frac{T^{n+1} - T^n}{\Delta t} + \theta \cdot K_{(T^{n+1})} T^{n+1} = F_{(T^{n+1})} - (1 - \theta) K_{(T^{n+1})} T^n \quad (7)$$

where the matrix $C_{(T^{n+1})}$ is the capacitance matrix, T^n is the nodal vector for the temperature at the time instant t_n , $K_{(T^{n+1})}$ is the conductivity matrix, and $F_{(T^{n+1})}$ is the vector of the thermal load. The vector of the thermal load may be defined according to boundary conditions represented in Figure 10.

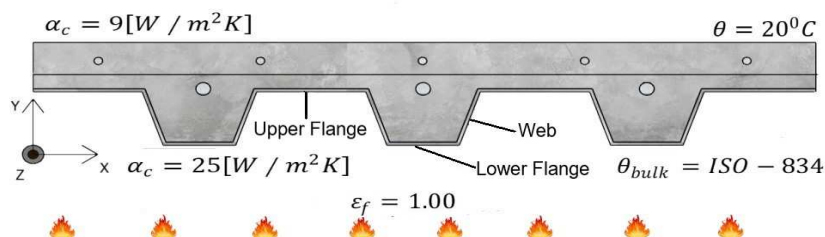


Fig. 10 – Composite Slabs Boundary Conditions.

The finite element mesh is generally used to model solids in which, the heat flux by conduction is the predominant heat transfer method, while the radiation and convection are imposed through boundary conditions. According to Eurocode 1991-1-2 [11], the initial temperature may be assumed to be 20°C and a convection coefficient $\alpha_c = 9$ [W/m²K] is applied at the unexposed surface, using a bulk temperature of 20°C, which includes the radiation effect. The exposed surface considers the convection coefficient $\alpha_c = 25$ [W/m²] and the flame emissivity

$\epsilon = 1$, both considering the bulk temperature following the standard fire ISO 834 [7]. The emissivity of both materials is considered to be 0.7.

The two-dimensional finite element model was developed in the software MATLAB, using the PDE Toolbox. Four faces were required for each slab, each one referring to its respective material, one for concrete, one for the rebar, one for the steel deck, and one for the air layer. The air layer is used to enhance the numerical results towards the experimental measurements developed during fire tests [4-6]. One finite element mesh is depicted in Figure 11 as an example for the trapezoidal geometry.

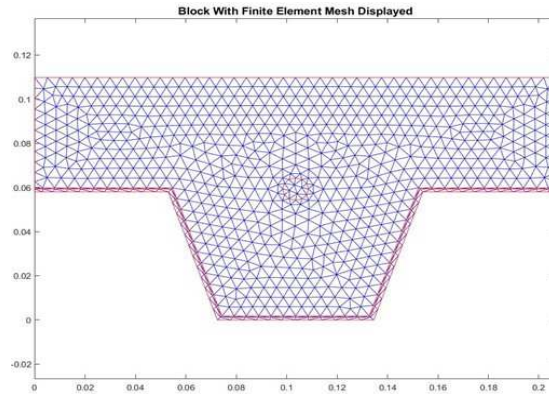


Fig. 11 – 2-D Finite Element Mesh.

This mesh is made with triangles, using linear interpolating functions and a complete Gauss integration scheme. These elements have three nodes, each with one degree of freedom (temperature). The convergence criterion used for the 2D analysis is based on a tolerance value of 10^{-4} for the temperature. The three-dimensional finite element model was developed in ANSYS. Three finite elements available in the Ansys library were selected for the model (SOLID70, LINK31, SHELL131). These elements were selected to meet the geometric conditions of each component of the composite slabs. The SOLID70 finite element was used to model the concrete. For the steel deck and to represent the debonding effect, the layered SHELL131 was adopted. This is a shell finite element generally used to represent thin structures. Finally, the one-dimensional LINK33 finite element was selected to represent the rebars and the steel mesh, see Figures 12-14.

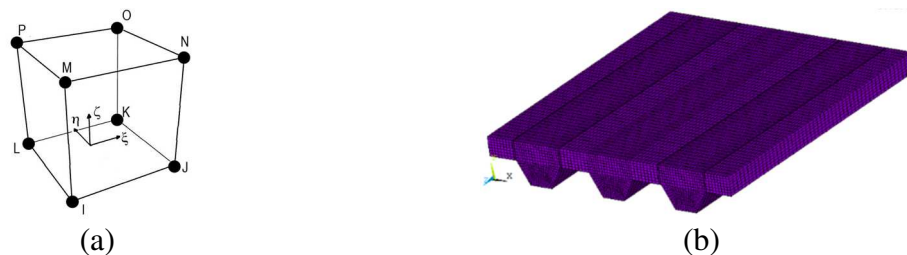


Fig. 12 – Finit element SOLID70: geometry (a) and application to concrete modeling (b).

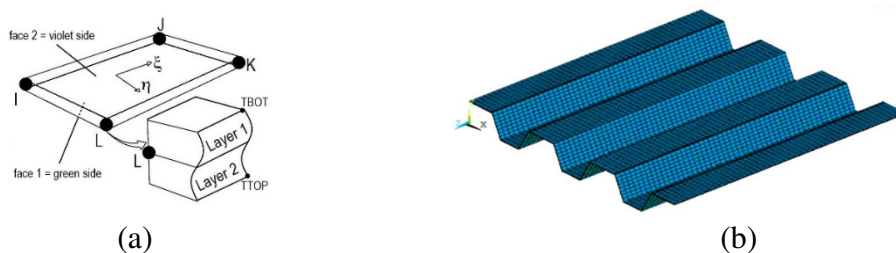


Fig. 13 – Finite element SHELL 131: geometry (a) and application to steel deck modeling (b).

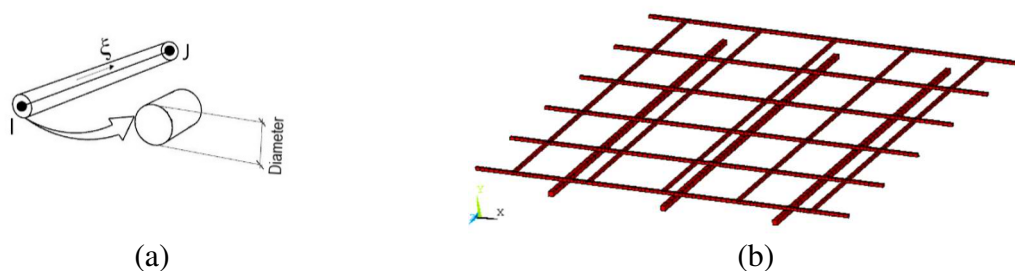


Fig. 14 – Finite element LINK 33: geometry (a) and application to anti-crack mesh modeling (b).

The convergence criterion adopted for the simulations developed using ANSYS software was based on the “heat flow ” with a reference value 10^{-6} [W] and a tolerance 10^{-3} . For each time step, the solution converges when in two sequential iterations, the relative error associated with the heat flow is less than or equal to the reference value multiplied by the tolerance value.

TEMPERATURE RESULTS

The results of the two-dimensional thermal analysis performed in MATLAB are presented, which were also compared against the three-dimensional results obtained through ANSYS. For both cases, each result of the thermal component thermal analysis comes from the average of the nodal temperatures along the length of each component (upper flange, web, and lower flange). Two different models have been developed. The numerical model (N,air) includes an air-gap layer of 0.5 mm to account for the debonding effect, and the numerical model (N) neglects this effect (air-gap is 0 mm).

Figure 15 and Figure 16 highlight the debonding effect (air gap) on the average temperature of each component. Numerical results (N) are compared with the simplified results (S). Figure 15 presents the thermal behavior of the trapezoidal Polydeck 59s slab with $h_1=50$ mm NWC thickness, and Figure 16 presents the thermal behavior of the re-entrant Multideck 50 slab with $h_1=60$ mm LWC thickness. In both examples, the numerical results with the air gap are closer to the simplified results (S), obtained by Annex D of Eurocode 1994-1-2.

Thus, through the 2D analysis of the composite slabs with steel deck, one can note a significant difference between the numerical results (N) and the results obtained by the simplified calculation method (S). The results obtained by the simplified method are always below the numerical results, which can be considered unsafe.

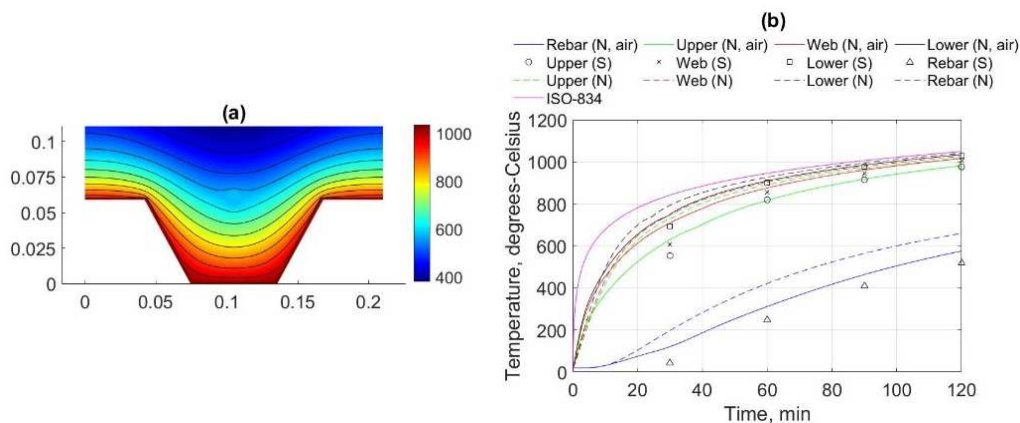


Fig. 15 – (a) Polydeck 59s Cross-section at 120 min, (b) Temperature evolution for each component obtained by simplified (S) and numerical (N) methods, considering the “air-gap” (N, air).

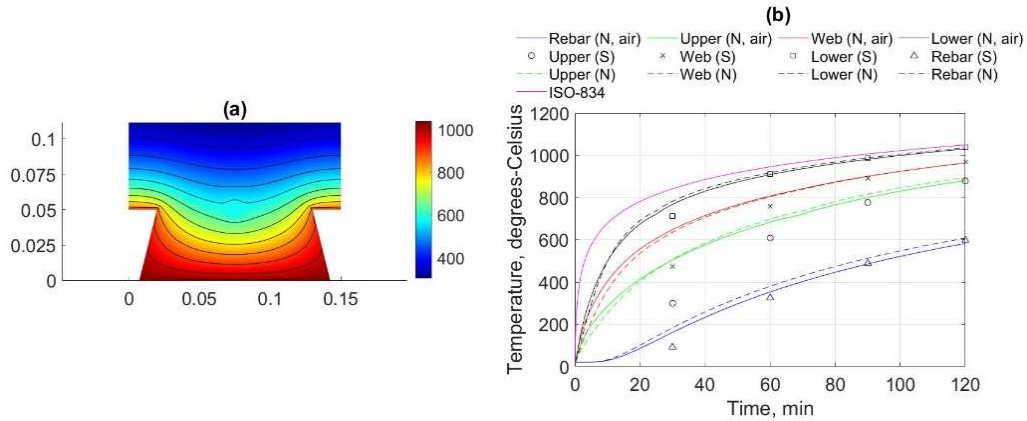


Fig. 16 – (a) Multideck 50 Cross-section at 120 min, (b) Temperature evolution for each component obtained by simplified (S) and numerical (N) methods, considering the “air-gap” (N, air).

The 3D numerical results were determined with ANSYS to introduce the effect of the mesh on the compressed concrete component and to compare the results with the 2D model. Figure 17 shows the temperature curves with an air-gap layer of 0.5 mm. Figure 17(a) represents the temperature distribution at 7200s, and Figure 17(b) represents the temperature history of the main components when using Polydeck 59S slab with $h_1=90$ mm NWC thickness.

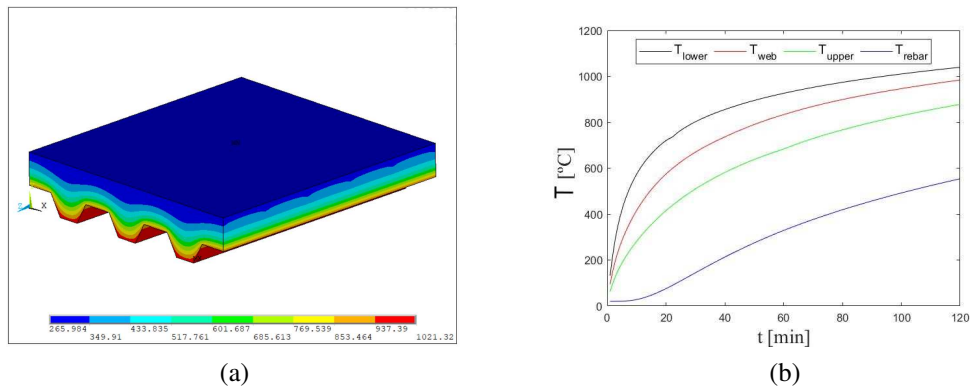


Fig. 17 – (a) Temperature field at 7200s, (b) Temperature evolution of Polydeck 59S slab with $h_1=90$ mm and NWC.

Similar results were obtained for composite slabs with Lightweight Concrete (LWC). Figure 18 represents the results for the Multideck 50 re-entrant composite slab, with $h_1=90$ mm LWC thickness. Figure 18(a) represents the temperature field at 7200s, and Figure 18(b) represents the temperature history curves for all the main components.

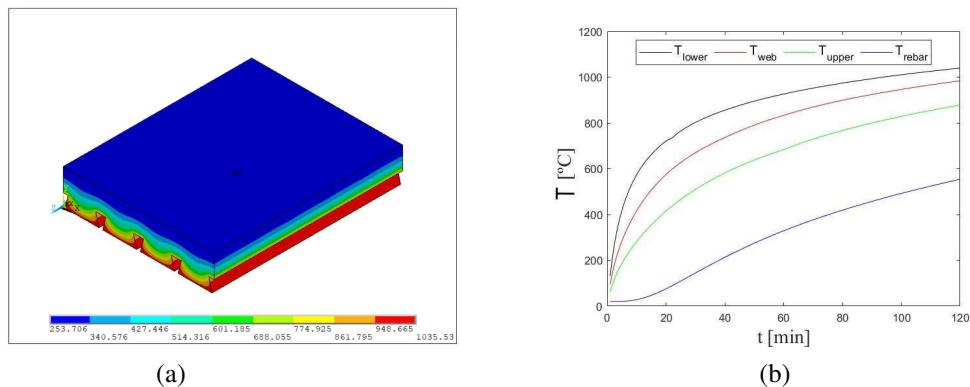
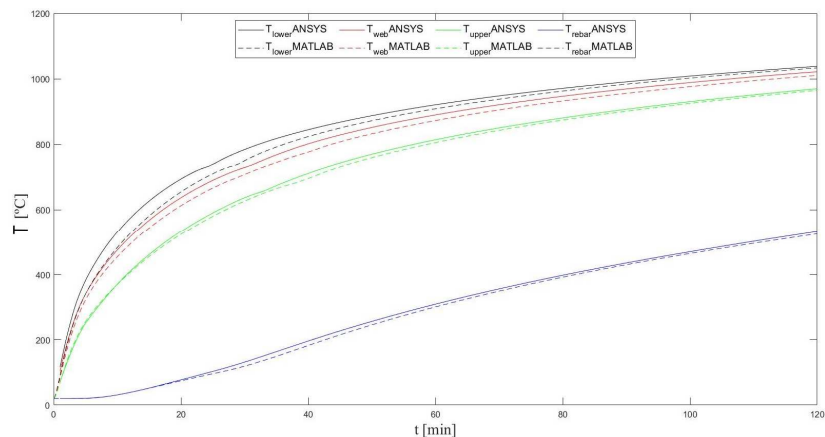
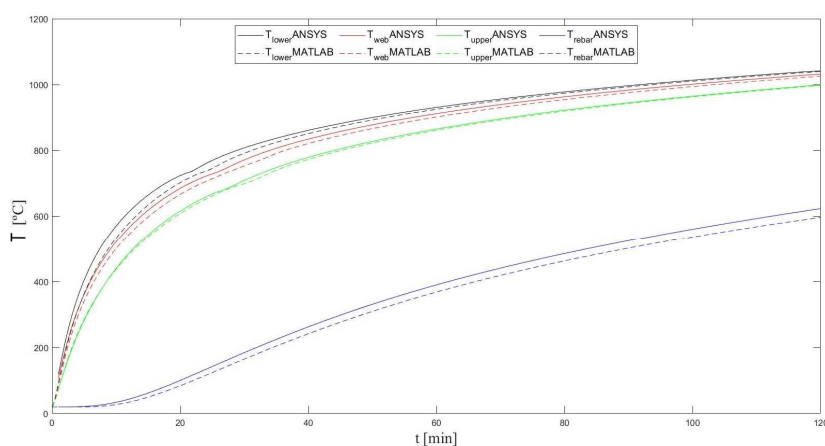


Fig. 18 – (a) Temperature field at 7200s, (b) Temperature of Multideck 50 slab with 90 mm and LWC.

Then a comparison between 2-D and 3-D results was performed. Fig. 19(a) presents this comparison for the Polydeck 59S composite slab with $h_1=90\text{mm}$ thickness in NWC, while Fig. 19(b) presents the same approach in LWC.



(a)



(b)

Fig. 19 – Comparison Between 2-D and 3-D results (a) NWC, (b) LWC.

As shown in Figure 19, the temperature curves obtained using ANSYS are in good agreement with those obtained through MATLAB. But it is noteworthy that there is a slight difference between the methods due to the difference between the models, when using different types of finite elements, and convergence methods.

NEW DEVELOPMENTS FOR THE SIMPLIFIED METHOD

Based on temperature results, a new proposal is presented to estimate the temperature in the steel deck components and on the rebars, for each specific time defined by fire rating. Additionally, new coefficients were also estimated for fire rating time of 45 min. The Eq. 8 and Eq. 9, presents the new proposal to calculate the steel temperature components for the steel deck and rebar, respectively.

$$\theta_a = \left(b_0 + b_1 \frac{1}{l_3} + b_2 \frac{A}{L_r} + b_3 \varphi + b_4 \varphi^2 \right) b_5 \quad (8)$$

$$\theta_s = \left(c_0 + c_1 \frac{u_3}{h_2} + c_2 z + c_3 \frac{A}{L_r} + c_4 \alpha + c_5 \frac{1}{l_3} \right) c_6 \quad (9)$$

Where θ_a is the temperature of the lower flange, web, or upper flange, θ_s is the temperature of reinforcement, l_3 is the width of the upper flange, φ is the view factor of the upper flange, A is the concrete volume of the rib per meter of rib length, L_r is the exposed area of the rib per meter of rib length, u_3 is the distance between the rebar and the lower flange, z is the indication of the rebar position in the rib, and α is the web angle.

Table 3 presents the new c_i coefficients, and Table 4 the new b_i coefficients, based on the best fit with the numerical results. The coefficients were determined using the nonlinear least-squares method. This method consists of minimizing the sum of the squared deviations between the temperatures proposed by Eqs. 8 or 9 and those obtained through numerical simulations.

Table 3 – New c_i coefficients proposal.

Concrete	Fire Resistance [min]	c0	c1	c2	c3	c4	c5	c6 (Reen.)	c6 (Trap.)
NWC	45min	1119,424	-238,565	-225,829	-4,848	0,753	-799,074	0,967	1,074
	60min	1222,465	-248,614	-236,672	-4,994	1,042	-924,710	0,924	1,085
	90min	1340,456	-256,056	-235,114	-5,301	1,390	-1267,220	0,914	1,085
	120min	1366,326	-238,609	-228,442	-4,797	1,677	-1326,630	0,911	1,085
LWC	30min	869,303	-133,293	-228,595	-0,699	0,481	-314,874	0,941	1,088
	45min	1136,412	-186,526	-257,236	-3,387	1,059	-607,138	0,929	1,080
	60min	1389,993	-240,148	-284,908	-6,077	1,635	-899,743	0,924	1,088
	90min	1408,635	-239,078	-265,938	-5,447	2,244	-917,988	0,911	1,090
	120min	1410,768	-229,550	-251,558	-4,436	2,471	-906,106	0,916	1,083

Table 4 – New b_i coefficients proposal.

Concrete	Fire Resistance [min]	Component	b0	b1	b2	b3	b4	b5 (Re-entrante)	b5 (Trapezoidal)
NWC	45min	Upper	741,682	-1662,508	-2,983	95,627	-185,548	0,806	1,196
		Web	635,365	-722,241	-3,293	689,525	-344,987	1,116	0,938
		Lower	65,720	-1003,213	-0,842	3413,949	-819,347	1,848	0,404
	60min	Upper	784,199	-1203,728	-2,348	86,101	-151,088	0,827	1,174
		Web	755,223	-829,652	-2,906	558,943	-346,533	1,040	0,979
		Lower	566,697	-2695,557	-2,234	1564,899	-639,673	1,420	0,709
	90min	Upper	857,473	-841,761	-1,561	64,953	-108,279	0,860	1,140
		Web	867,775	-957,472	-2,199	471,327	-338,061	1,010	0,995
		Lower	832,185	-2674,885	-1,739	842,270	-459,529	1,187	0,873
	120min	Upper	919,406	-680,486	-1,135	46,638	-82,886	0,886	1,114
		Web	954,715	-948,415	-1,817	346,186	-266,592	0,995	1,006
		Lower	949,386	-2414,930	-1,646	619,924	-373,440	1,116	0,913
LWC	30min	Upper	707,052	-1333,093	-2,679	114,271	-181,238	0,846	1,155
		Web	617,936	-285,157	-2,183	489,380	-233,828	1,072	0,952
		Lower	602,463	-2041,618	-1,401	673,167	-124,325	1,297	0,815
	45min	Upper	778,304	-977,333	-1,999	80,970	-131,232	0,869	1,131
		Web	729,593	-420,919	-1,935	451,609	-269,052	1,037	0,979
		Lower	712,807	-2130,545	-1,228	668,287	-261,018	1,216	0,865
	60min	Upper	824,177	-623,389	-1,327	47,611	-81,232	0,882	1,118
		Web	807,934	-557,537	-1,664	433,574	-300,574	1,016	0,988
		Lower	785,929	-2206,045	-1,007	724,299	-397,923	1,159	0,879
	90min	Upper	906,500	-478,614	-0,913	32,668	-60,857	0,911	1,089
		Web	926,942	-653,858	-1,359	289,299	-229,586	0,995	1,005
		Lower	925,111	-1831,257	-0,984	485,781	-308,685	1,084	0,930
120min	Upper	964,213	-399,340	-0,651	19,790	-43,724	0,929	1,071	
	Web	997,217	-628,997	-1,070	186,448	-152,413	0,990	1,010	
	Lower	1010,532	-1554,441	-0,917	309,836	-195,989	1,052	0,954	

In order to verify the differences between the results obtained with the current version of the Eurocode 1994-1-2 (EC), the results from numerical results (NUM), and the results from the new calculation proposal (NP), a graph is presented. Figure 20 presents the results for each component (upper flange, web, lower flange and rebar) using NWC, while Figure 21 presents this comparison for composite slabs using LWC.

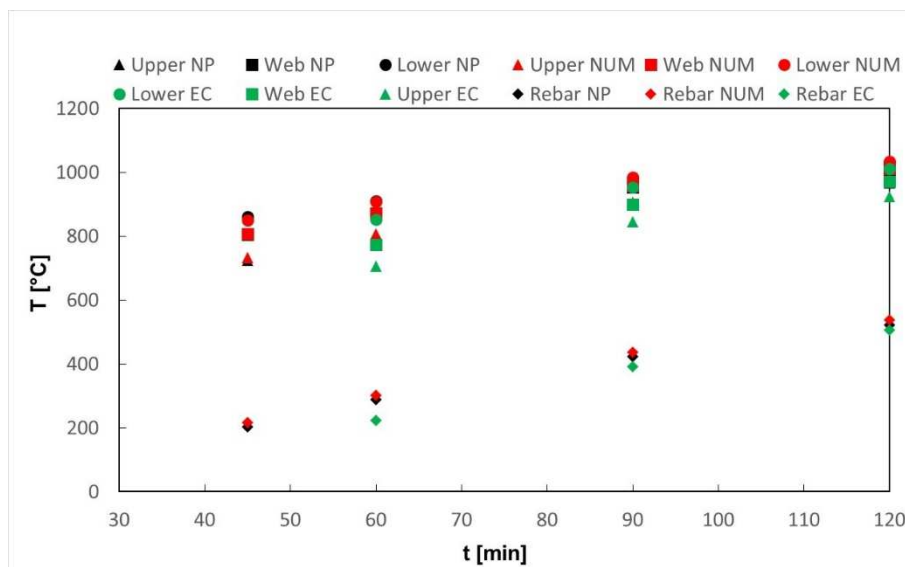


Fig. 20 - Temperature for the composite slabs Polydeck 59S with NWC.

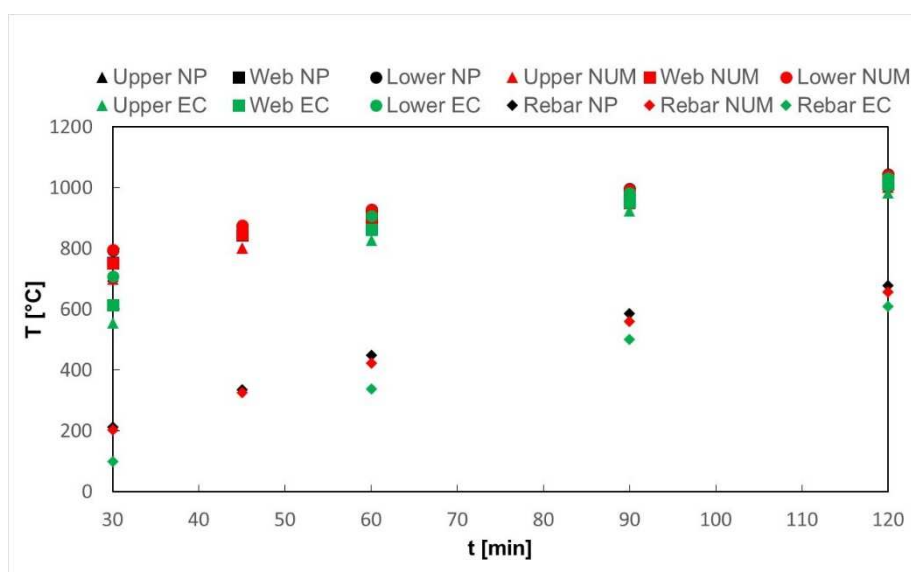


Fig. 21 - Temperature for the composite slabs Bondek with LWC.

Through the graphs presented in Figure 20 and Figure 21, one can see that the temperatures obtained by the new proposal are very similar to those obtained through parametric studies, demonstrating that, there is an improvement in the accuracy of the results, when using the new proposal.

SIMPLIFIED METHOD: BENDING RESISTANCE FOR SAGGING MOMENT

After the accurate temperature prediction for each fire rating class, the sagging moment has been calculated and compared to the bending resistance at room temperature. The ratio will provide the new bending resistance reduction factor ($M_{f_i,t,Rd}/M_{Rd}$) for the sagging moment. Figures 22-25 present the reduction factors for all the composite slabs, when using NWC and LWC. These graphs also highlight the difference between the results obtained with the current version of the EN1994-1-2 and the new proposal.

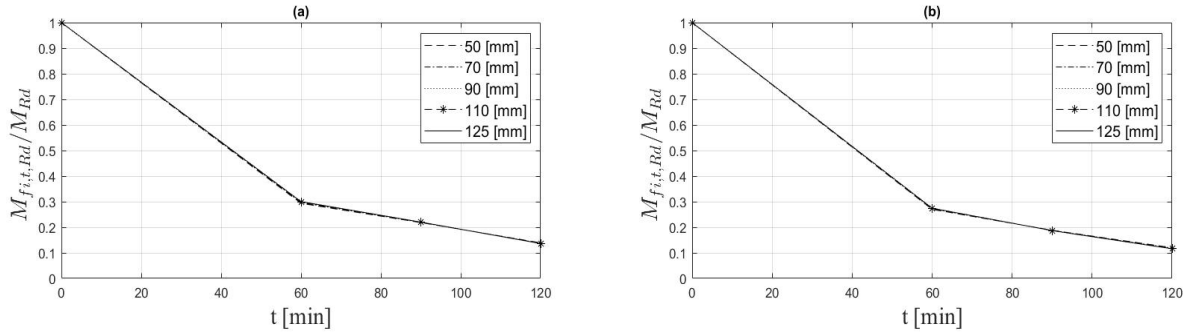


Fig. 22 – Bending resistance reduction factor for Confraplus 60 slab with NWC: (a) EN 1994-1-2, (b) new proposal.

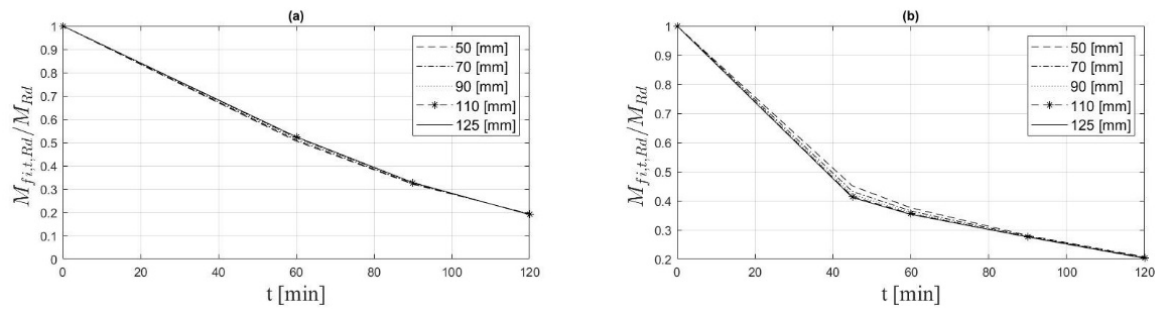


Fig. 23 – Bending resistance reduction factor for Multideck 50 slab with NWC: (a) EN 1994-1-2, (b) new proposal.

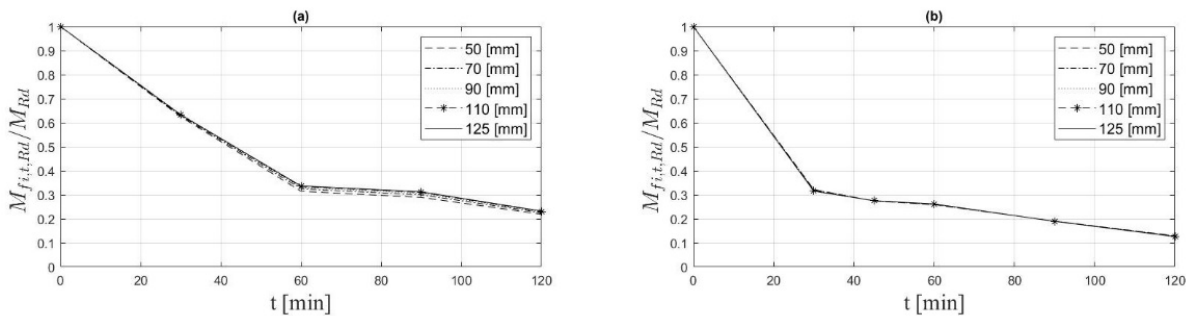


Fig. 24: Bending resistance reduction factor for Polydeck 59S slab with LWC: (a) EN 1994-1-2, (b) new proposal.

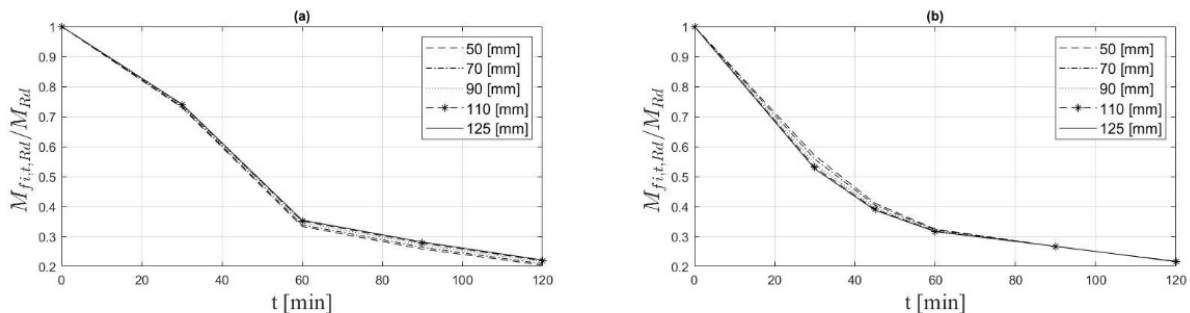


Fig. 25: Bending resistance reduction factor for Bondek slab with LWC: (a) EN 1994-1-2, (b) new proposal.

In all cases, without exceptions, the reduction is higher when using the new calculation proposal. Through a quantitative approach, it is possible to ensure that the reduction is in the order of 3% to 20% for most of the fire rating times. However, for the smaller fire ratings (30 min and 45 min), the reduction is even higher, reaching 50% for the LWC with trapezoidal steel decks.

CONCLUSIONS

This work aimed to present a new calculation proposal by introducing an alternative calculation formula to the Annex D of Eurocode 1994-1-2 [3], and also presenting new coefficients. This new proposal improved the temperature prediction of steel deck components and rebar, and introduced new parameters that allow the calculation of temperatures for a fire rating period of 45 min.

The results have been previously validated with experimental results [4-6]. A comparison was also made between the 2D model using Matlab and the 3D model using ANSYS. The temperature results obtained from ANSYS were higher on average, between 10 and 15 °C and, and in special cases reaching 35 °C. The differences presented between the developed numerical models are attributed to some factors: the difference in the geometry of the finite elements used, the difference in the types of finite elements used and the difference in the convergence parameters.

The new proposal was compared with the results provided by the Annex D of Eurocode 1994-1-2. The variations are on average of 6% for the trapezoidal slabs and 10% for the re-entrant slabs. However, for the smallest fire ratings (30 min), this variation is even bigger, reaching 40% for the case of re-entrant composite slabs.

The performance of the new calculation proposal was also evaluated concerning the load-bearing criterion (R). The maximum bending moment under fire ($M_{f,t,Rd}$) was calculated for all the composite slabs geometry, considering different h_1 thickness and concrete types. This value was then divided by the maximum bending resistant moment of the slab at room temperature (M_{Rd}), allowing the calculation of the load bearing reduction factor. The results prove the existence of a reduction in the order of 3% to 20% for most of the fire rating times. However, this effect is increased for the smaller fire ratings (30 and 45 min), reaching 50% for the case of LWC in trapezoidal steel decks.

REFERENCES

- [1] Cooke, G. M. E., LKawason, R. M. & Newman, G. M. Fire Resistance of Composite Deck Slabs. 1988.
- [2] Guo, S. Experimental and numerical study on restrained composite slab during heating and cooling. Journal of Constructional Steel Research 69, 95–105. ISSN: 0143- 974X (2012). DOI: <http://dx.doi.org/10.1016/j.jcsr.2011.08.009>.
- [3] CEN, EN 1994-1-2: Design of composite steel and concrete structures. Part 1-2: General rules - Structural fire design. Brussels, 2005.

- [4] Paulo A. G. Piloto, Carlos Balsa, Fernando Ribeiro, Ronaldo Rigobello, Computational Simulation of the Thermal Effects on Composite Slabs under Fire Conditions, *Math. Comput. Sci.*, 2020. DOI: <https://doi.org/10.1007/s11786-020-00466-0> .
- [5] Paulo A.G. Piloto, Carlos Balsa, Lucas M.C. Santos, and Érica F.A. Kimura (2020). Effect of the load level on the resistance of composite slabs with steel decking under fire conditions. *Journal of Fire Sciences*, vol. 38, Issue 2, pp: 212-232, 2020. DOI: <https://doi.org/10.1177/0734904119892210> .
- [6] Paulo A. G. Piloto, Carlos Balsa, Fernando F. Ribeiro, Ronaldo Rigobello. Three-Dimensional Numerical Analysis on the Fire Behaviour of Composite Slabs with Steel Deck, Chapter 2, pp: 12-30, 2020, *Advances in Fire Safety Engineering*, Springer, Lecture Notes in Civil Engineering, DOI: <https://doi.org/10.1007/978-3-030-36240-9>.
- [7] ISO, “ISO 834-1: Fire Resistance Tests - Elements of Building Construction - Part 1: General Requirements.” International Organization for Standardization, Switzerland, p. 25, 1999.
- [8] CEN, EN 1992-1-2: Design of concrete structures - Part 1-2: General rules - Structural fire design. Brussels, 2004.
- [9] CEN, EN 1993-1-2: Design of steel structures - Part 1-2: General rules - Structural fire design. Brussels, 2005.
- [10] Cengel, Y. & Ghajar, A. *Heat and Mass Transfer, Fundamentals & Application*, Fifth Edition in SI Units 496. ISBN: 9780471457282 (2015).
- [11] CEN, EN 1991-1-2: Eurocode 1: Actions on structures - Part 1-2: General actions - Actions on structures exposed to fire. Brussels, 2002.